7

Engineering DNA Switches for DNA Computing Applications

Dominic Lauzon[1], *Guichi Zhu*[2], *and Alexis Vallée-Bélisle*[1,2]

[1] *Université de Montréal, Laboratory of Biosensors & Nanomachines, Département de Chimie, 1375, Ave Thérèse-Lavoie-Roux Montréal, Montréal, QC H2V 0B3, Canada*
[2] *Université de Montréal, Institut de Génie Biomédical, Département de Pharmacologie et Physiologie, 2900, boul Édouard-Montpetit, Montréal, QC H3T 1J4, Canada*

7.1 Introduction

Through billions of years of evolution, living organisms have developed a myriad of finely tuned nanomachines to monitor changes in their environment. In order to respond to these changes, or input, cells rely on biomolecules that undergo structural changes in the presence of specific chemical or physical inputs (e.g. temperature, pH, small molecules, proteins and other macromolecules, or even viruses and bacteria) [1]. Upon activation, these structure-switching molecules can then trigger one or multiple output mechanisms to efficiently react to the perturbation previously detected. It can be, for example, by changing the function of other biomolecules, by increasing/decreasing gene expression, by opening/closing transmembrane proteins, or by triggering the self-assembly of biomolecules [2, 3]. Examples of natural structure-switching molecules, also called biomolecular switches, include the regulating protein calmodulin that changes its structure and activity following calcium binding (four Ca^{2+} binding sites), which transduces a change in cell function by regulating downstream effectors [4, 5]. Another example of biomolecular switches are the G protein-coupled receptors, a membrane protein family containing over 800 identified members, that control cellular fate via binding-induced structural variation triggers by various chemical inputs (light, odorant molecules, hormones, etc.) [6, 7].

Inspired by the efficiency of natural switches, chemists and engineers have begun to synthesize molecular systems that take advantage of these nanoscale switching mechanisms. For example, some have created switches using light-, binding-, and current-induced structural changes [1, 8–10]. One superstar molecule to create structure-switching nanosystems is DNA. This is due to its high programmability (i.e. folding and binding energies) combined with its

DNA- and RNA-Based Computing Systems, First Edition. Edited by Evgeny Katz.

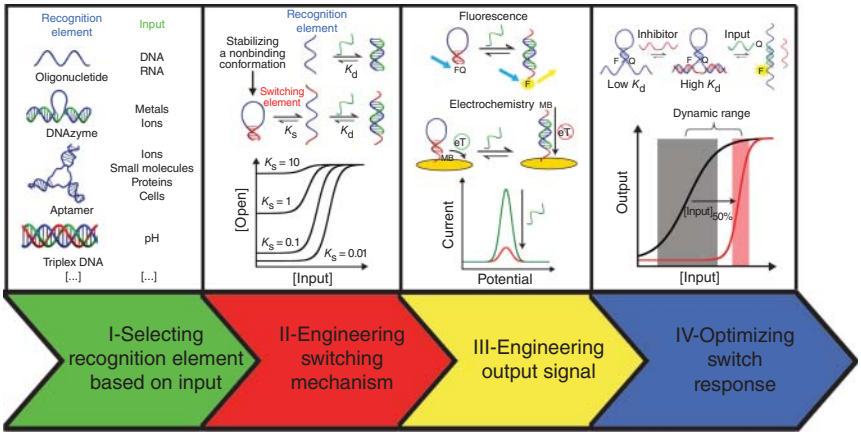

Figure 7.1 Engineering steps of DNA switches. (I) DNA can adopt a wide range of nanostructures acting as recognition elements for specific chemical input. (II) The selected recognition element must, therefore, be converted into a structure-switching nanosystem by stabilizing a nonbinding conformation. (III) Analytical readouts, such as fluorescence or current, can be introduced to record the input-induced structure switching. (IV) Different strategies exist to optimize the dose–response profile of a switch to better suit the desired application. Source: From Harroun et al. [1]. Reproduced with the permission of Royal Society of Chemistry.

ease of synthesis and relative ease of chemical conjugation to a wide range of molecules and nanomaterials [1]. DNA, for example, can specifically bind to its complementary sequence and can also fold into a wide range of nanostructures (e.g. i-motif, G-quadruplex, aptamers, DNA triplex, hairpin, etc.) that can selectively interact with other class of chemical species (e.g. ions, small molecules, proteins, etc.) [8, 9]. Given these features, DNA switches have thus found many applications in DNA computing enabling, for example, the creation of molecular automaton that can play games [11], perform square root calculations [12], function as a security system [13], and perform cancer theranostics [13, 14] as well as molecular diagnostics [15].

To rationally develop DNA switches into logic circuits, one must first think about the inputs that will trigger structure switching and then choose recognition elements accordingly (Figure 7.1I). Once chosen, the recognition elements must be converted into structure-switching molecules by stabilizing a nonbinding conformation (Figure 7.1II). In this design phase, one should also consider how different recognition elements can be combined to obtain a switch that responds to more than one input molecule. Then, an output function must be introduced to enable an analytical readout of the switch (Figure 7.1III). Finally, and only in some cases, the switching behavior is not always optimal for the desired application and thus needs to be optimized to better suit it (Figure 7.1IV). In this chapter, we summarize the major steps and considerations required to create DNA switches, from scratch, and we further discuss the rationale behind the design and creation of DNA computing systems based on DNA switches [1, 16].

7.2 Selecting Recognition Element Based on Input

The initial step of designing DNA switches for DNA computing applications is to select an appropriate recognition element for the desired input species (Figure 7.1I). Inputs are typically classified into three categories, including physical phenomena (e.g. temperature and light), chemical stimuli (e.g. protons, metal and nonmetal ions, small molecules, nucleic acids, and proteins), and biological units (e.g. viruses, cells, and bacteria). Through programming the stability of a DNA fold by its length or GC/AT base pair composition, for example, one can create a variety of temperature-induced DNA switches that can be activated at various specific temperatures [17–19]. Light-sensitive DNA switches that employ chemically modified DNA strands have also been explored [20–22]. As is well known, DNA can selectively bind its complementary sequence, which has led to the development of fluorescence-producing structure-switching molecular beacons by Kramer and Tyagi in 1996 [23]. Some DNA recognition elements can also selectively bind non-nucleic acid molecules. For example, a triplex DNA strand has been designed through both Watson–Crick and Hoogsteen base pairing interactions to determine a solution's pH value [24]. The i-motif is another noncanonical DNA structure that is stabilized under acidic pH conditions due to the protonation of cytosine and can thus serve as a pH sensor [25]. DNA G-quadruplex structures can be formed or stabilized in the presence of potassium ions (K^+) [26], while mercury ions (Hg^{2+}) [27] and silver ions (Ag^+) [28] stabilize DNA conformations containing thymine–thymine and cytosine–cytosine base pair mismatches, respectively. DNAzymes are another widely used recognition element for metal ions. These latter can often act as specific cofactors to catalyze the cleavage of nucleic acid substrate strands (e.g. Mg^{2+} [29], Pb^{2+} [30], and UO_2^{2+} [31]). Short single-stranded DNA (ssDNA) or RNA sequences can also be selected *in vitro* by the systematic evolution of ligands by exponential enrichment (SELEX) [32]. These sequences enable the binding of small molecules and proteins with a typical high affinity and specificity (see aptamers) [33]. Finally, the biological units of viruses, cells, and bacteria also can be recognized by their respective aptamer sequences that specifically bind to the viral proteins and cell membrane proteins [34–37].

For DNA computing applications, the recognition element often needs to process multiple inputs. To do so, the DNA recognition elements must interact with two (or more) inputs that are often chemically distinct. Sometimes, such DNA strands already exist. This is the case, for example, of one thrombin aptamer that requires the presence of K^+ to fold into a G-quadruplex in order to bind the thrombin protein [26]. Therefore, this DNA recognition element can be used to sense both K^+ and thrombin. However, this exception is somewhat peculiar, as most of the time the design of multiple input recognition elements must be engineered from scratch by combining two (or more) elements together. For example, an aptamer sequence was introduced into the loop section of a clamp-like triplex DNA, thereby rendering the binding of the aptamer with its input pH dependent [38]. Similarly, an aptamer sequence was introduced into the arm section of a DNAzyme, thus making the switch sensitive toward both the aptamer's input and the metallic cofactor [39]. Another strategy is to fuse together two relevant DNA

recognition elements into a stem-loop, which renders its opening sensitive to the presence of both inputs simultaneously [40]. Overall, selection of the right recognition element for detection of multiple inputs becomes only limited by one's creativity to merge various DNA recognition elements into a broader nanosystem.

7.3 Engineering Switching Mechanisms

Efficient signaling of artificial nanoswitches is often related to their capacity to undergo large conformational changes upon binding of the desired input (Figure 7.1II). For example, fluorescence- or electrochemical-producing switches generally require large conformational change in order to generate high output signaling (e.g. Figure 7.1III). Some DNA nanostructures already spontaneously undergo large conformational changes upon binding. For example, the i-motif undergoes large conformational changes upon protonation of cytosine, going from a nonstructured random coil conformation to a well-defined intercalated nanostructure [25, 41]. DNA input molecules will also drastically affect the structure of their host DNA receptors upon binding by triggering a structure change from a flexible unfolded ssDNA conformation to a more rigid double helix conformation. On the other hand, many DNA structures offer limited structure-switching behavior upon binding to their input molecules. This is often the case with aptamers, where the screening effort via SELEX does not consider structural motifs in the selection process and thus typically leads to DNA sequences that are more stable in their binding-competent state [42, 43]. To overcome this limitation, strategies have been developed to introduce (or enhance) conformational changes upon binding of the input [44]. These strategies mostly rely on the population-shift mechanism, which involves the stabilization of a nonbinding conformation to improve the magnitude of conformational changes [5]. This mechanism is typically thought to proceed through a three-state equilibrium that involves a first switching equilibrium between the nonbinding and the binding-competent states along with the binding equilibrium of the input that can only interact with the binding-competent state (Figure 7.2a). The presence of the input will thus trigger the switching of the DNA by shifting its equilibrium toward the bound state through the gain of new favorable interactions between the input molecule and the DNA.

To ensure good switching, the nonbinding state must remain the most favorable conformation of the DNA sequence in the absence of the input (i.e. lowest energy state). Designing such switching systems thus requires a good understanding of the folding free energy (ΔG) of both the nonbinding and binding-competent states. In order to do so, websites like NUPACK [45], Mfold [46], and IDT SciTools [47] enable user-friendly estimation of the folding free energy of DNA secondary structures based on Watson–Crick interactions. Unfortunately, such websites or software do not yet exist for more complex DNA tertiary structures such as G-quadruplexes, i-motifs, and aptamers. Therefore, the design of these systems mostly relies on experimental characterization of their free energy. Validation and characterization of switching (or binding)

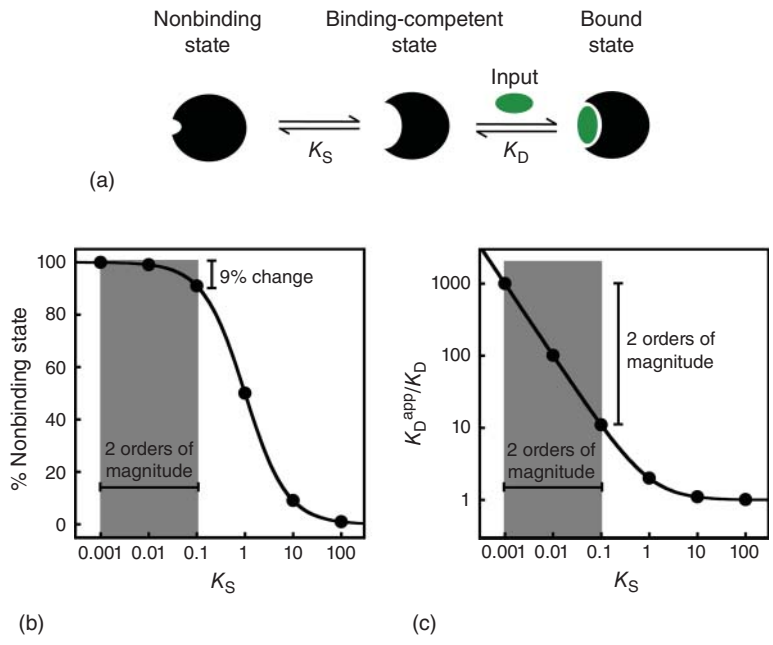

Figure 7.2 (a) Cartoon representation of the population-shift mechanism. The switch is in equilibrium between the nonbinding and binding-competent states (K_S), and this equilibrium is shifted toward the bound state (K_D) upon addition of the input. To ensure a large population of DNA in the nonbinding state without drastically altering the apparent binding affinity of our input (K_D^{app}), K_S must remain lower than 0.1 because (b) high K_S does not provide enough population of DNA in the nonbinding state, thus ultimately leading to an insufficient population shift to be accurately monitored, while (c) a lower K_S will result in a drastic energetic penalty for the binding of the input (K_D^{app}).

free energy can be easily measured either through urea [48] or temperature [49] denaturation curves. To achieve good switching behavior, the equilibrium switching constant (K_S = [binding-competent state]/[nonbinding state]), which is related to the free energy (ΔG_S) through Eq. (7.1), must remain below 0.1. This ensures a low background with a large signal change because at least 90% of the DNA will, in the presence of its input, switch from the nonbinding state to the binding-competent state (Figure 7.1II). One must keep in mind that employing a $K_S \gg 0.1$ leads to a system wherein the population of DNA in the nonbinding state is too low, thus ultimately leading to not enough switches remaining to generate a population shift large enough to be accurately monitored. In contrast, over-stabilizing the nonbinding conformation via a $K_S \ll 0.1$ will increase the concentration of input needed to trigger the switching (K_D^{app}) relative to the intrinsic affinity between the input and the DNA recognition element (K_D) (see Eq. (7.2)) [5]. To illustrate this relationship more quantitatively, a switch with a K_S of 0.1 provides maximal change in population of 90.9% with only a 10-fold penalty in observed affinity, whereas a K_S of 0.001 only improves the population shift by 9% (90.9% vs. 99.9%) while drastically increasing the energetic penalty of binding by 2 orders of magnitude (10-fold vs. 1000-fold) (Figure 7.2b,c). As we

will see in step IV (optimizing switch response), optimizing of the switching constant K_S can also be used to optimize the switch response within a specific input concentration range.

$$\Delta G_S = -RT \ln(K_S) \tag{7.1}$$

$$K_D{}^{app} = K_D \frac{(1 + K_S)}{K_S} \tag{7.2}$$

Many strategies exist to stabilize a DNA recognition motif into a nonbinding state (Figure 7.3). A widely used strategy is to modify the DNA recognition element into a stem-loop (Figure 7.3a) [50]. This can be achieved by introducing two short complementary sequences at the 3′ and 5′ extremities that constrain the entire DNA sequence to adopt a stem-loop conformation different from the one it adopts when bound to the input molecule (i.e. the linear conformation adopted in a duplex DNA vs. the specific tertiary structure of an aptamer sequence). The new interactions between the input and the recognition element

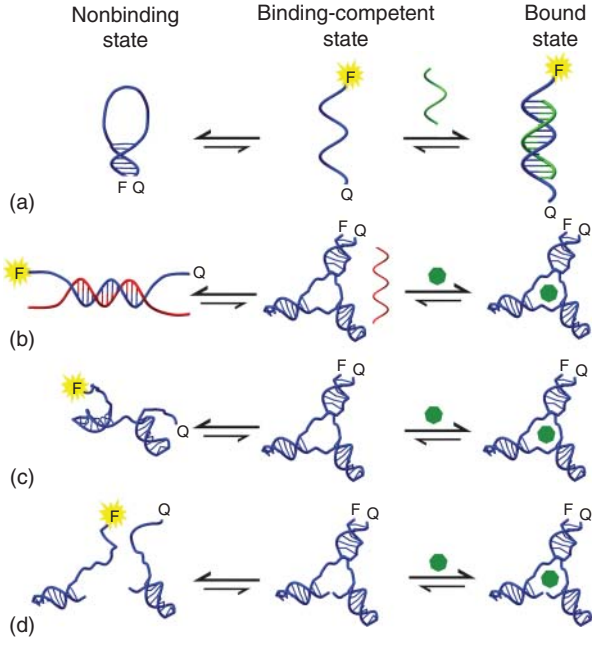

Figure 7.3 Based on the population-shift model, different strategies exist to stabilize a DNA recognition element into a nonbinding conformation. (a) Short complementary sequence can be added at the 5′ and 3′ extremities of the recognition element, which will bend it into a molecular beacon. (b) A complementary sequence of our recognition element (in red) can be added to promote the formation of a DNA duplex. (c) Nucleotides can be mutated or deleted to disrupt interactions present in the binding-competent state, thus rendering the nonbinding state more favorable. (d) Splitting the recognition element in half also destabilizes the binding-competent state. Source: From Harroun et al. [1]. Reproduced with the permission of Royal Society of Chemistry.

will therefore act as the driving force to disrupt the Watson–Crick base pairs formed in the stem. A second convenient strategy to create a structure-switching mechanism consists of inserting a DNA strand (red) that is complementary to the DNA recognition element (Figure 7.3b). This duplex can still sample the binding-competent state and can therefore be displaced toward the binding state by the input. A third strategy involves a mutational (or deletion) method, where some nucleotides are changed (or removed) in order to destabilize the binding-competent state, thus rendering the nonbinding state more favorable (Figure 7.3c). Of course, mutation (or deletion) should not be performed with nucleotides that are known to be important for the selectivity and specificity of the recognition element. A good understanding of the secondary structure of the DNA recognition element is thus required to avoid any perturbation of the binding surface. A fourth strategy requires one to split the DNA recognition element into two DNA sequences that will be brought together upon addition of the input (Figure 7.3d). As with the mutational/deletion strategy, splitting should be avoided in regions that are relevant for the binding of the input. Breaking the phosphodiester bond at such relevant positions may disrupt interactions that cannot be retrieved when dimerization is triggered by the input.

As mentioned previously, DNA computing typically requires the processing of information obtained from multiple inputs. To access information based on two molecular inputs, the population-shift model can be readily adapted to consider the effect of an allosteric effector on the affinity between the switch and the initial input (Figure 7.4a). We have previously described [51] how DNA allosteric effectors can be readily designed to stabilize/destabilize the binding-competent state (or nonbinding state) of a switch. Allosteric activation happens when an effector molecule binds and stabilizes the switch into the binding-competent state, thus increasing K_S (Figure 7.4a, top). This makes it easier for the input to bind the switch and reduces the midpoint ($K_D{}^{input}$) toward a lower concentration of input (Figure 7.4b). This behavior is well modeled by Eq. (7.3), where K_S is the switching constant, K_D is the dissociation constant between the input and the switch, K_A is the dissociation constant between the activator and the switch, $[A]$ is the concentration of activator, and α is the ratio of dissociation constants in the presence and absence of activator [51]. It is important to note that the midpoint can only be shifted until a certain threshold defined by α. In other words, further addition of an activator will not push the midpoint toward a lower concentration, but rather, it will limit it to a specific threshold as defined by the affinity of the input for a switch fully bound by the activator. Therefore, one must optimize the activator to enable a change in input affinity that is large enough to create a measurable change in the output signal. Likewise, allosteric inhibition happens when the effector molecule binds and stabilizes the nonbinding state, thus reducing K_S (Figure 7.4a, bottom). This makes it harder for the input to bind, as it increases the energetic penalty of binding, thus increasing the midpoint ($K_D{}^{input}$) toward a higher concentration of input (Figure 7.4c). This behavior is well modeled by Eq. (7.4), where K_I is the dissociation constant between the inhibitor and the switch and $[I]$ is the concentration of inhibitor [51]. In this case, no threshold is observed, as a higher concentration of inhibitor always leads to a higher midpoint.

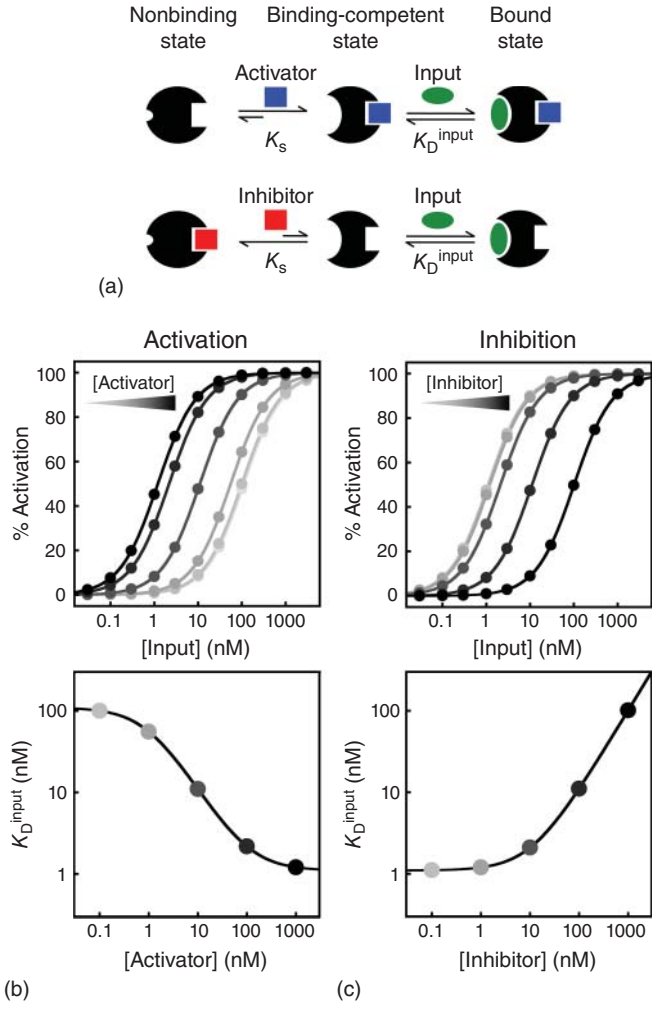

Figure 7.4 Creating switches based on the population-shift model for double input detection. (a) The population-shift model can readily be adapted to consider the effect of a new input called an effector (shown as a square). We call the effector an activator when the molecule (blue square) stabilizes the binding-competent state, and conversely, we call it an inhibitor when the molecule (red square) stabilizes the nonbinding state. (b) The presence of an activator increases the affinity of the switch for our initial input until a certain threshold defined by the affinity of that input for a switch fully bound by the activator. (c) On the other hand, the presence of an inhibitor reduces the affinity of the switch for the initial input by increasing the energetic penalty of binding related to lowering K_S.

$$K_D^{\text{input}} = K_D \left(\frac{1 + K_S}{K_S} \right) \left(\frac{1 + \frac{[A]}{K_A}}{1 + \frac{[A]}{\alpha K_A}} \right) \tag{7.3}$$

$$K_D^{\text{input}} = K_D \left(\frac{1 + K_S \left(\frac{K_I}{K_I + [I]} \right)}{K_S \left(\frac{K_I}{K_I + [I]} \right)} \right) \tag{7.4}$$

Allosteric inhibition and activation mechanisms enable the introduction of a second variable (i.e. the effector) that renders simple two-variable Boolean operations possible. Using allosteric activation, for example, one can easily produce an OR gate, where the presence of an activator and/or the input can stabilize the switch into the binding-competent state (Figure 7.5a). In this scenario, if one wants to detect a specific concentration of at least one molecule (input and/or activator), it is imperative that each molecule have their concentration higher than their respective dissociation constant ($K_A <$ [activator], $K_D^{\text{input}} <$ [Input]). This ensures that a good shift in population happens when at least one of the two molecules is present. This strategy has recently been employed to activate the catalytic activity of a DNAzyme (Figure 7.5b) [52]. Here, the DNAzyme has been transformed into a switch by incorporating a DNA strand that sequesters the catalytic loop, thus preventing its activity. Two input DNA strands were also designed to be complementary to the sequestering DNA strand. Therefore, the activity of the DNAzyme can be recovered by adding either one of the inputs, both of which cause the displacement of the sequestering DNA strand and the correct folding of the DNAzyme. This highlights how the switch design can easily be combined with allosteric effectors to enable the creation of well-controlled logic gate.

Another logic gate that can be created using an allosteric activator is the AND gate (Figure 7.5c). This gate provides an output signal only when all inputs are present. In contrast with the OR gate, each molecule must have their concentration lower than their respective dissociation constant ($K_A >$ [activator], $K_D^{\text{input}} >$ [Input]). This ensures that both molecules cannot individually activate the switch and that the presence of each is required to stabilize the switch into the binding-competent state. For that to happen, one must program the concentration of activator such that it does not, alone, significantly shift the population of switches toward the binding-competent state ([activator] $< K_A$), but still enhances the binding of the input significantly. This strategy has been incorporated into a DNAzyme by intentionally mutating one arm of the DNAzyme switch (blue arm) such that the substrate cannot efficiently bind (Figure 7.5d) [53]. In this case, a DNA effector strand (blue strand) was also rationally introduced to bind to the mutated section and allow the recovery of the missing Watson–Crick base pairs for the substrate, thus enhancing the affinity for the substrate. The DNAzyme is, therefore, only active when both inputs (effector and substrate) are present. Here, we can appreciate how the mutation strategy was exploited to create a logic gate by simply using one input to enable the recovery of the native interactions, therefore favoring the binding of the second input.

Finally, using an allosteric inhibiter, INHIBIT gates become readily achievable (Figure 7.5e). Such gates only provide an output signal when one input of interest is present alone. Therefore, the affinity of the input must be lower than the concentration that it is intended to detect ($K_D^{\text{input}} <$ [Input]) in order to provide

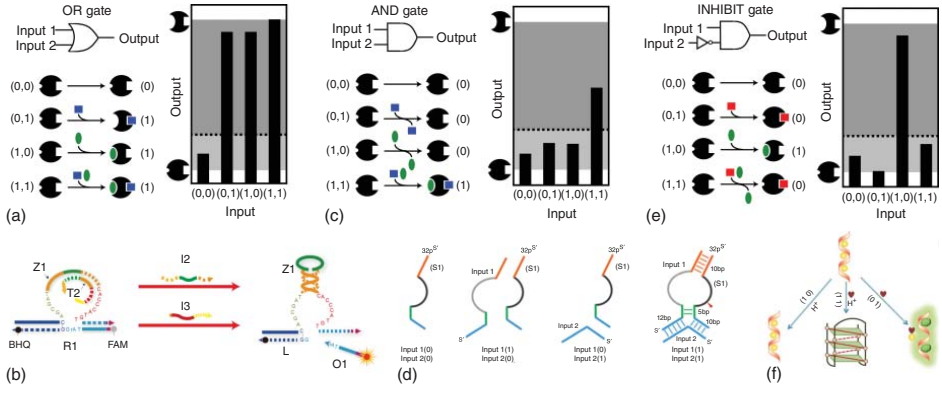

Figure 7.5 Exploiting allosteric effectors to create logic gates. (a) Using allosteric activation, one can produce an OR gate where the presence of an activator (blue square) and/or the input (green circle) can stabilize the switch into the binding-competent state. (b) This strategy has been exploited using a DNAzyme by adding a sequestering strand (T2) into the catalytic loop. The activity can be retrieved by the addition of either one of the inputs (I2 and I3), which are both complementary to the sequestering strand. (c) Allosteric activation can also be used to create an AND gate if the activator (blue square), when bound, does not significantly increase the affinity for the input (green circle). (d) This strategy has been adapted with a DNAzyme by intentionally mutating one arm of the DNAzyme switch (blue arm). Therefore, the presence of both DNA strands is required to reform the DNAzyme and retrieve its activity. (e) Allosteric inhibition can easily be adapted to create an INHIBIT gate. In this case, an allosteric inhibitor (red square) stabilizes the switch into the nonbinding state. Therefore, only the input alone (green circle) can activate the switch and produce a signal. (f) This strategy was exploited using a silver-deposited DNA that can detect the presence of cysteine (heart shape) by removing the silver deposition (yellow circle) from the DNA scaffold through the formation of Ag—S bonds. However, the DNA recognition element was also built to respond to a change of H^+, the allosteric inhibitor, when the silver depositions are removed by the cysteine. It does so by stabilizing the switch into a nonbinding state (i.e. a i-motif), thus rendering the switch only active in the presence of cysteine alone. Data from panel a, c, and e are simulated using the population-shift model with Eqs. (7.3) and (7.4). Source: (Panel b) From Zheng et al. [52]. Reproduced with the permission of Oxford University Press; (Panel d) From Furukawa and Minakawa [53]. Reproduced with the permission of Royal Society of Chemistry; (Panel f) From Gao et al. [54]. Reproduced with the permission of Royal Society of Chemistry.

a good change in population for that input. Also, the inhibitor must be programmed such that its presence prevents the binding between the input and the switch by favoring the nonbinding state. This can be done by using a concentration of inhibitor higher than its K_I and that is also large enough to significantly decrease the affinity of the input. This strategy has been used many times by simply introducing an inhibitor molecule (e.g. DNA strand or small molecule) that either favors the formation of the nonbinding state of the switch or prevents the analytical readout when bound to the switch (Figure 7.5f) [53–55]. For example, a switch made using the RET proto-oncogene and silver deposition was used to detect the presence of cysteine by removing the silver deposition from the DNA scaffold through the formation of Ag—S bonds [54]. The DNA is then free to bind thioflavin T, which results in a fluorescent signal. However, the addition of protons, the inhibitor, into the mixture favors the folding of the DNA into an i-motif, thus preventing its detection by thioflavin T.

Many examples of these different logic gates have been developed in recent years. Pei et al., for example, have developed a DNA tetrahedron with logic response by incorporating dynamic sequences into the edges of the nanostructure (Figure 7.6a) [56]. Here, a small hairpin containing a 5′-CCGC-3′/5′-GCGG-3′ stem ($\Delta G = -2.1\,\text{kcal mol}^{-1}$ at 37 °C using Mfold, $K_S = 0.033$) was introduced into one edge, providing an expected 97% population shift with only a 30-fold penalty in observed affinity. Each input was engineered to bind half of the loop and invade a section of the stem. In order to correctly fold the edge of the tetrahedron, the presence of both inputs (AND gate) is required to compensate the lost of stability caused by the disruption of the stem. This versatile switching DNA tetrahedron was further adapted for the detection of intracellular ATP in living cells by incorporating an ATP aptamer in one of the edges. Our second example illustrates how switching thermodynamics can have a huge impact on the activity of a switch. Here, Zhang et al. have created a nano-assembly containing a multi-hairpin motif engineered to produce logic response in the presence of microRNAs (Figure 7.6b) [57]. The microRNAs cannot bind with one of their DNA construct (called L0) because it contains hairpins that were too stable (ΔG of $-6.2\,\text{kcal mol}^{-1}$, $K_S = 4 \times 10^{-5}$ and $-8.4\,\text{kcal mol}^{-1}$, $K_S = 1 \times 10^{-6}$) and therefore drastically increases the energetic penalty of binding by at least 5 orders of magnitude. A second construct (called L3) with less stable hairpins (ΔG of $-3.4\,\text{kcal mol}^{-1}$, $K_S = 4 \times 10^{-3}$ and $-5.2\,\text{kcal mol}^{-1}$, $K_S = 2 \times 10^{-4}$) has shown promising results by producing a logic response in the presence of three different microRNAs. This study highlights the importance of engineering switches with optimal thermodynamics. In our last example, Chen and Zeng used the sequestration and splitting strategy to adapt an ATP aptamer and a thrombin aptamer into many different logic switches [58]. The first design introduces a signaling DNA strand that is complementary to both aptamers' sequences (Figure 7.6c). Therefore, the presence of any of the inputs triggers the displacement of that signaling DNA duplex, thus leading to a NOR gate. This same strategy can be used to create a NAND gate by using two signaling DNA strands that will individually sequester each aptamer (Figure 7.6d). Also, the splitting strategy was also used to create a recognition element and a signaling strand that each contain both sections of the ATP and thrombin aptamers. This

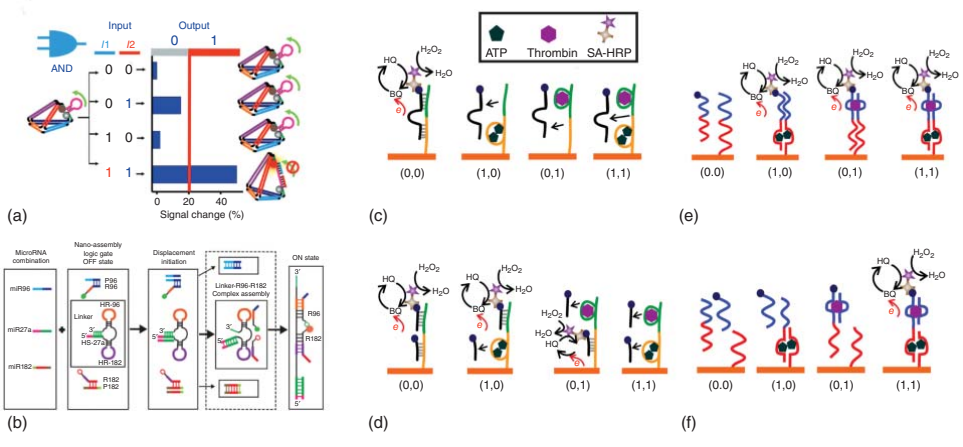

Figure 7.6 Examples of logic gate created using the strategies discussed in this chapter. (a) Here, a small stem-loop containing 4GC base pairs was introduced at one edge of a tetrahedron to make its opening dependent on the binding of two inputs that bind each half of the loop. (b) A microRNA logic gate was built using a multi-hairpin motif. (c) A new recognition element was built by fusing an ATP aptamer and a thrombin aptamer together. A signaling strand was then designed to be complementary to that new recognition element. Therefore, the presence of any input will displace the signaling strand, thus resulting in a NOR gate. (d) Cutting that same signaling strand in two halves creates two smaller signaling strands that can individually bind to each aptamer's section. Therefore, each signaling strand can be displaced by their respective inputs, thus creating a NAND gate. (e) The splitting strategy was also used to create a recognition element and a signaling strand that each contain both sections of the ATP and thrombin aptamers. This leads to an OR gate, where the presence of at least one input is required to bring both strands together. (f) This strategy was rendered more complex by splitting the system into three different strands, where the presence of both inputs is required to bring all strands together, thus creating an AND gate. Source: (Panel a) From Pei et al. [56]. Reproduced with the permission of John Wiley & Sons; (Panel b) From Zhang et al. [57]. Reproduced with the permission of Royal Society of Chemistry; (Panels c–f) From Chen and Zeng [58]. Reproduced with the permission of Elsevier.

leads to the creation of an OR gate, where the presence of at least one input is required to pay the energetic price of bringing back together the two split sections of the aptamers (Figure 7.6e). This splitting strategy has also been used to create an AND gate by splitting the DNA sequence into three components, where the presence of both inputs is required to pay the energetic price (Figure 7.6f).

7.4 Engineering Logic Output Function Response

Selection of effective logic output mechanism plays a critical role in DNA switch design (Figure 7.1III). Fortunately, it is convenient to engineer the output signal for DNA switches due to the general ease and simplicity of chemically labeling DNA strands with reporter molecules. Among the various types of output signals, fluorescence spectroscopy and electrochemical analysis are two most widely employed methods used for DNA switches in DNA computing applications. Fluorescence possesses the advantages of high sensitivity, homogeneous assays, excellent reproducibility, and easy operation [59]. For example, by virtue of distance change-induced Förster resonance energy transfer (FRET), a variety of fluorescent methods have been developed to record the conformational changes of DNA switches [60]. Typically, a fluorophore and a quencher are added at the extremity of stem-loop DNA switches (5′ and 3′ terminals – see, for example, the molecular beacon [23]), and a very low fluorescence signal is obtained in the absence of a DNA input due to the significant energy transfer between the fluorophore and quencher. Upon addition of a DNA sequence complementary to the loop sequence, the stem structure is opened, and a strong fluorescence signal is generated due to the separation of the fluorophore and quencher. Alternatively, nanomaterials including gold nanoparticles [61] and graphene oxides [62] can also be employed as a quencher in DNA switches. Moreover, nucleotide analogs with specific fluorescent properties, such as 2-aminopurine [63], can also be added into the DNA strand as a fluorescent reporter for the study of DNA structure and dynamics [64]. In comparison to the classic fluorophore/quencher pairs, 2-aminopurine is less susceptible to photobleaching because its excitation wavelength is outside of the visible light range [65]. In order to decrease the synthesis cost of chemically modified fluorescent reporters, label-free methods (e.g. fluorescent intercalators) have also been explored for DNA switches [66].

Electrochemical analysis is the other commonly used output signal to monitor the conformational change of DNA switches. Typical electrochemical techniques include cyclic voltammetry (CV), alternative current voltammetry (ACV), differential pulse voltammetry (DPV), and square wave voltammetry (SWV) [67]. These electrochemical methods have attracted increasing attention due to their high sensitivity, good specificity, low cost, and especially insusceptibility to the matrix effects of biological samples [68]. The electrochemical output signal depends on the specific binding between the DNA switches and the specific input molecules in order to conduct electron transfer at the electrode surface, thereby generating an electrochemical output signal. Since 2003, Plaxco's lab

has described many strategies based on the binding-induced conformational changes of DNA switches in an electrochemical format [69, 70]. As a proof of principle, a redox-labeled DNA switch is first immobilized on a gold electrode surface through a Au—S bond to form a stem-loop structure [69], which is analogous to the fluorescent molecular beacon reported by Kramer [23]. In the absence of target DNA, the stem-loop structure of the DNA switch brings the redox element into close proximity with the electrode surface and generates a high electrochemical current. However, in the presence of target DNA, the stem-loop structure is opened via the complementary hybridization between the DNA switch and input DNA, which leads to a significant decrease of the electrochemical current since the redox element is pushed away from the surface. Small molecules and proteins are also used as input molecules to trigger the conformational change of DNA switches on the electrode surface [71–74]. Various logic gates have also been designed using similar electrochemical strategies [75]. Of note, label-free electrochemical methods have attracted attention due to their inherent simplicity and low cost. For example, electrochemical impedance spectroscopy (EIS) is a promising label-free strategy that measures electron transfer resistance change between ssDNA and dsDNA (or aptamer and target–aptamer complex) in the presence of a redox reporter such as ferricyanide [76]. Typically, an increase in electron transfer resistance is observed in dsDNA [77] (or target–aptamer complex [78–80]) due to the stronger negative charge repulsion between ferricyanide and dsDNA (or target–aptamer complex). Besides fluorescence spectroscopy and electrochemical analysis, colorimetry [81], chemiluminescence [82], and surface-enhanced Raman scattering (SERS) [83] have also been explored as output signals in DNA switches.

7.5 Optimizing Switch Response

Introducing switching behavior to the chosen DNA recognition element does not always lead to switches that are functional within the desired input concentration range. For this reason, the dose–response profile of the switch must be optimized to obtain a relevant dynamic range (Figure 7.1IV) [16]. Two simple parameters can be used to describe the response profile of a switch, namely, (i) the midpoint and (ii) the dynamic range. The midpoint characterizes the concentration of input needed to produce a 50% change in output signal ($[\text{Input}]_{50\%}$, Eq. (7.5)). This parameter is generally referred as the apparent dissociation constant (K_D^{app}, or simply K_D) because it represents the inflection point of the sigmoidal dose–response curve. The simplest method to tune the midpoint of a switch has already been discussed previously (Section 7.3) and involves the stabilization of the nonbinding conformation consistent with the population-shift mechanism (see Eq. (7.2)).

$$\text{Midpoint} = K_D^{app} = [\text{Input}]_{50\%} \tag{7.5}$$

$$\text{DR} = \frac{[\text{Input}]_{90\%}}{[\text{Input}]_{10\%}} = 81^{(1/n_H)} \tag{7.6}$$

The dynamic range (DR), also referred as the sensitivity, defines the range of input concentrations needed to produce structure switching. It can be numerically assessed by the ratio of concentrations that give 90% and 10% output signal ($DR = [Input]_{90\%}/[Input]_{10\%}$). It can also be assessed through the empirical Hill factor (n_H), which is linked with the DR by Eq. (7.6) [84]. Typical dose–response curves have a dynamic range of 81-fold ($n_H = 1$). A simple strategy to extend the dynamic range is to use multiple switches that possess differing midpoints (Figure 7.7a, top). To achieve that, a good understanding of the input/output response of each individual switch is required to determine the optimal ratio of switches to build a switch system providing an optimal "linear" extended dynamic range. For example, by mixing in an equimolar ratio of three switches with midpoints at 1, 10, and 100 nM, respectively, the dynamic range can be extended by almost an order of magnitude from 81-fold to 791-fold without affecting the linearity of the response (Figure 7.7a, bottom). An easy method to obtain multiple variants of the same switch is to introduce mutations or by deleting some of the nucleotides. This creates switches that will have lower affinity compared with the native switch. Using that strategy, the dynamic range of a cocaine switch system was extended by 330 000-fold by combining four different variants of the cocaine aptamer [85]. However, because this strategy uses switch variants of reduced affinity, the midpoint will therefore always be higher than the midpoint of the native switch. To overcome that limitation, it is possible to use an allosteric approach to create new switches that will have higher affinity (activation) or lower affinity (inhibition) [51]. This strategy has been used to create a mixture of Hg^{2+} molecular beacons that are activated over a 333-fold dynamic range and that remain centered around its natural K_D of 16 μM [86].

We have previously discussed strategies that enable one to extend the dynamic range of switches. However, in DNA computing, it is often more relevant to engineer all-or-none switches (i.e. switches that are activated over a narrow dynamic range). Such systems can be engineered by exploiting mechanisms used in regulatory networks [87]. One of these strategies involves the introduction of a molecule (called a depletant) that will sequester the input (Figure 7.7b, top). It is important that this new molecule, which can be a small molecule, DNA, protein, or others, has a higher affinity toward the input ($K_D{}^{dep} < K_D{}^{input}$) to prevent the accumulation of free input. As long as there is depletant molecule available, the input will not be able to activate the switch until reaching a certain concentration threshold defined by the total concentration of depletant in the system (Figure 7.7b, bottom). Above that concentration, further addition of input leads to a large increase in free input that can immediately activate the switch, thus producing a "pseudo-cooperative" dose–response curve (i.e. a small dynamic range). It has been demonstrated that a key parameter to achieve a small dynamic range is the stoichiometric binding parameter, which corresponds to the ratio of depletant concentration over the affinity of the switch for the input ($[depletant]/K_D{}^{input}$) [88]. This parameter dictates whether mass action will favor the depletant-induced sequestration (>1) or the formation of free input (<1). It has been shown that the dynamic range starts increasing monotonically when the stoichiometric binding parameter becomes higher than unity. Simulation of

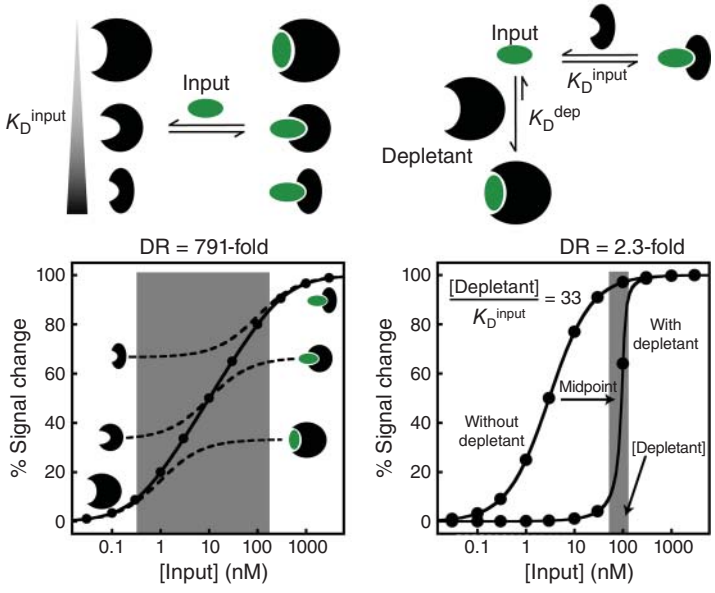

Figure 7.7 (a) Two or more switches with different affinities for the input can be combined to enlarge the dynamic range. For example, using three different switches with midpoints of 1, 10, and 100 nM enables one to enlarge the dynamic range to 791-fold without affecting the linearity of the response. (b) The sequestration mechanism can be used to achieve an ultrasensitive response at a threshold concentration corresponding to the depletant concentration. For example, using a stoichiometric binding parameter of 33 enables one to decrease the dynamic range up to 2.3-fold.

that mechanism predicts that it is theoretically possible to achieve a Hill factor as high as 21.6 (DR = 1.22-fold) when using a stoichiometric binding parameter of 10 000 [88]. However, narrowing the dynamic range using that strategy comes with the trade-off of increasing the midpoint of the curve (Figure 7.7b, bottom). Nonetheless, by using this strategy, many researchers were able to engineer all-or-none switches that can, for example, activate by a 4-fold change in input concentration when using TATA-binding protein, 3-fold when using the cocaine aptamer, and even 1.5-fold when using a molecular beacon [85, 89].

7.6 Perspective

In this chapter, we have summarized various strategies for engineering DNA switches and their applications for DNA computing. Such switches are likely to drive many innovations in the fields of medicine, green chemistry, and nanotechnology, but several challenges lie ahead before realizing this promise beyond laboratory-scale prototypes [90]. One such challenge is developing switches that achieve sufficient specificity and selectivity (i.e. only triggered

by a specific molecular input) even in complex conditions or environments (such as whole blood, soil, etc.). To that end, we believe that expending the DNA code with other artificial nucleotides should greatly contribute to creating more specific recognition elements [91, 92]. Another challenge consists of better characterizing and optimizing DNA switch systems to obtain their innate structural and dynamic profiles. Such information would provide the rational basis to better optimize the switch's function and response behavior. With this in mind, we believe that novel tools to characterize the switch's thermodynamic signature (see Ref. [48]) and tune it, using simple and inexpensive strategies (such as employing inhibitors or activators [51]), should greatly contribute to making design strategies more rational and quantitative. Concerning switch kinetics, it is also important to note that activation and deactivation of DNA switches using a DNA trigger remains relatively slow, which limits applications in DNA computing. More specific challenges to move beyond laboratory-scale prototypes include optimizing the accuracy (through calibration against a standard), stability, repeatability, and reproducibility of DNA switch systems [90]. *In vivo* applications will also require a better understanding of the mechanisms underlying intracellular uptake, trafficking, and nanotoxicology [93], in addition to the characterization of their pharmacokinetic properties. Finally, a better understanding of large-scale production of DNA-based systems for better yields and lower costs [94] is mandatory to scale-up laboratory or pilot technologies to reach the production and commercialization stages.

Acknowledgments

This research was conducted through a Natural Sciences and Engineering Research Council of Canada Discovery Grants (A.V.-B.) and as part of the TransMedTech Institute's activities thanks, in part, to funding from the Canada First Research Excellence Fund. A.V.-B. is Canada Research Chair in Bioengineering and Bionanotechnology, Tier II, D.L. acknowledges a 3rd cycle scholarship from the Fonds de Recherche du Québec – Nature et technologies (FRQNT), and G.Z. acknowledges a 3rd cycle scholarship from TransMedTech. The authors thank Scott Haroun for useful comments on the manuscript.

References

1 Harroun, S.G., Prévost-Tremblay, C., Lauzon, D. et al. (2018). *Nanoscale* 10: 4607–4641.
2 Ma, C.-W., Zhou, L.-B., and Zeng, A.-P. (2018). Engineering biomolecular switches for dynamic metabolic control. In: *Synthetic Biology – Metabolic Engineering* (eds. H. Zhao and A.-P. Zeng), 45–76. Cham: Springer International Publishing.
3 Wieland, M. and Fussenegger, M. (2012). *Annu. Rev. Chem. Biomol. Eng.* 3: 209–234.
4 Chin, D. and Means, A.R. (2000). *Trends Cell Biol.* 10: 322–328.

5 Vallée-Bélisle, A., Ricci, F., and Plaxco, K.W. (2009). *Proc. Natl. Acad. Sci. U.S.A.* 106: 13802.
6 Lagerström, M.C. and Schiöth, H.B. (2008). *Nat. Rev. Drug Discovery* 7: 339–357.
7 Rosenbaum, D.M., Rasmussen, S.G.F., and Kobilka, B.K. (2009). *Nature* 459: 356–363.
8 Krishnan, Y. and Simmel, F.C. (2011). *Angew. Chem. Int. Ed.* 50: 3124–3156.
9 Wang, F., Liu, X., and Willner, I. (2015). *Angew. Chem. Int. Ed.* 54: 1098–1129.
10 Harris, J.D., Moran, M.J., and Aprahamian, I. (2018). *Proc. Natl. Acad. Sci. U.S.A.* 115: 9414.
11 Pei, R., Matamoros, E., Liu, M. et al. (2010). *Nat. Nanotechnol.* 5: 773–777.
12 Qian, L. and Winfree, E. (2011). *Science* 332: 1196.
13 Chen, J., Zhou, S., and Wen, J. (2015). *Angew. Chem. Int. Ed.* 54: 446–450.
14 Pei, H., Zuo, X., Zhu, D. et al. (2014). *Acc. Chem. Res.* 47: 550–559.
15 Engelen, W., Meijer, L.H.H., Somers, B. et al. (2017). *Nat. Commun.* 8: 14473.
16 Vallée-Bélisle, A., Ricci, F., and Plaxco, K.W. (2012). *J. Am. Chem. Soc.* 134: 2876–2879.
17 Ebrahimi, S., Akhlaghi, Y., Kompany-Zareh, M., and Rinnan, A. (2014). *ACS Nano* 8: 10372–10382.
18 Gareau, D., Desrosiers, A., and Vallée-Bélisle, A. (2016). *Nano Lett.* 16: 3976–3981.
19 Ke, G., Wang, C., Ge, Y. et al. (2012). *J. Am. Chem. Soc.* 134: 18908–18911.
20 Asanuma, H., Ito, T., Yoshida, T. et al. (1999). *Angew. Chem. Int. Ed.* 38: 2393–2395.
21 Lubbe, A.S., Liu, Q., Smith, S.J. et al. (2018). *J. Am. Chem. Soc.* 140: 5069–5076.
22 Zhou, M., Liang, X., Mochizuki, T., and Asanuma, H. (2010). *Angew. Chem. Int. Ed.* 49: 2167–2170.
23 Tyagi, S. and Kramer, F.R. (1996). *Nat. Biotechnol.* 14: 303–308.
24 Idili, A., Vallée-Bélisle, A., and Ricci, F. (2014). *J. Am. Chem. Soc.* 136: 5836–5839.
25 Benabou, S., Aviñó, A., Eritja, R. et al. (2014). *RSC Adv.* 4: 26956–26980.
26 Kwok, C.K. and Merrick, C.J. (2017). *Trends Biotechnol.* 35: 997–1013.
27 Ono, A. and Togashi, H. (2004). *Angew. Chem. Int. Ed.* 43: 4300–4302.
28 Ono, A., Cao, S., Togashi, H. et al. (2008). *Chem. Commun.*: 4825–4827.
29 Breaker, R.R. and Joyce, G.F. (1995). *Chem. Biol.* 2: 655–660.
30 Liu, J. and Lu, Y. (2003). *J. Am. Chem. Soc.* 125: 6642–6643.
31 Liu, J., Brown, A.K., Meng, X. et al. (2007). *Proc. Natl. Acad. Sci. U.S.A.* 104: 2056–2061.
32 Tuerk, C. and Gold, L. (1990). *Science* 249: 505–510.
33 Jayasena, S.D. (1999). *Clin. Chem.* 45: 1628–1650.
34 Fang, X. and Tan, W. (2010). *Acc. Chem. Res.* 43: 48–57.
35 Gopinath, S.C., Hayashi, K., and Kumar, P.K. (2012). *J. Virol.* 86: 6732–6744.
36 Hamula, C.L., Zhang, H., Guan, L.L. et al. (2008). *Anal. Chem.* 80: 7812–7819.
37 Shangguan, D., Li, Y., Tang, Z. et al. (2006). *Proc. Natl. Acad. Sci. U.S.A.* 103: 11838–11843.
38 Zheng, J., Li, J., Jiang, Y. et al. (2011). *Anal. Chem.* 83: 6586–6592.

39 Achenbach, J.C., Nutiu, R., and Li, Y. (2005). *Anal. Chim. Acta* 534: 41–51.
40 Park, K.S., Seo, M.W., Jung, C. et al. (2012). *Small* 8: 2203–2212.
41 Abou Assi, H., Garavís, M., González, C., and Damha, M.J. (2018). *Nucleic Acids Res.* 46: 8038–8056.
42 Sullivan, R., Adams, M.C., Naik, R.R., and Milam, V.T. (2019). *Molecules* 24: 1572.
43 Cai, S., Yan, J., Xiong, H. et al. (2018). *Analyst* 143: 5317–5338.
44 Zhou, W., Jimmy Huang, P.-J., Ding, J., and Liu, J. (2014). *Analyst* 139: 2627–2640.
45 Zadeh, J.N., Steenberg, C.D., Bois, J.S. et al. (2011). *J. Comput. Chem.* 32: 170–173.
46 Zuker, M. (2003). *Nucleic Acids Res.* 31: 3406–3415.
47 Owczarzy, R., Tataurov, A.V., Wu, Y. et al. (2008). *Nucleic Acids Res.* 36: W163–W169.
48 Idili, A., Ricci, F., and Vallée-Bélisle, A. (2017). *Nucleic Acids Res.* 45: 7571–7580.
49 You, Y., Tataurov, A.V., and Owczarzy, R. (2011). *Biopolymers* 95: 472–486.
50 Wang, K., Tang, Z., Yang, C.J. et al. (2009). *Angew. Chem. Int. Ed.* 48: 856–870.
51 Ricci, F., Vallée-Bélisle, A., Porchetta, A., and Plaxco, K.W. (2012). *J. Am. Chem. Soc.* 134: 15177–15180.
52 Zheng, X., Yang, J., Zhou, C. et al. (2018). *Nucleic Acids Res.* 47: 1097–1109.
53 Furukawa, K. and Minakawa, N. (2014). *Org. Biomol. Chem.* 12: 3344–3348.
54 Gao, R.-R., Shi, S., Zhu, Y. et al. (2016). *Chem. Sci.* 7: 1853–1861.
55 Stojanovic, M.N., Mitchell, T.E., and Stefanovic, D. (2002). *J. Am. Chem. Soc.* 124: 3555–3561.
56 Pei, H., Liang, L., Yao, G. et al. (2012). *Angew. Chem. Int. Ed.* 51: 9020–9024.
57 Zhang, L., Bluhm, A.M., Chen, K.-J. et al. (2017). *Nanoscale* 9: 1709–1720.
58 Chen, J. and Zeng, L. (2013). *Biosens. Bioelectron.* 42: 93–99.
59 Schlichthaerle, T., Strauss, M.T., Schueder, F. et al. (2016). *Curr. Opin. Biotechnol.* 39: 41–47.
60 Huang, J., Yang, X., He, X. et al. (2014). *TrAC, Trends Anal. Chem.* 53: 11–20.
61 Jayagopal, A., Halfpenny, K.C., Perez, J.W., and Wright, D.W. (2010). *J. Am. Chem. Soc.* 132: 9789–9796.
62 Li, F., Huang, Y., Yang, Q. et al. (2010). *Nanoscale* 2: 1021–1026.
63 Jean, J.M. and Hall, K.B. (2001). *Proc. Natl. Acad. Sci. U.S.A.* 98: 37–41.
64 Millar, D.P. (1996). *Curr. Opin. Struct. Biol.* 6: 322–326.
65 Zhu, G., Liang, L., and Zhang, C.Y. (2014). *Anal. Chem.* 86: 11410–11416.
66 Feng, C., Dai, S., and Wang, L. (2014). *Biosens. Bioelectron.* 59: 64–74.
67 Tang, Y., Ge, B., Sen, D., and Yu, H.-Z. (2014). *Chem. Soc. Rev.* 43: 518–529.
68 Ronkainen, N.J., Halsall, H.B., and Heineman, W.R. (2010). *Chem. Soc. Rev.* 39: 1747–1763.
69 Fan, C., Plaxco, K.W., and Heeger, A.J. (2003). *Proc. Natl. Acad. Sci. U.S.A.* 100: 9134–9137.
70 Lubin, A.A. and Plaxco, K.W. (2010). *Acc. Chem. Res.* 43: 496–505.
71 Xiao, Y., Lubin, A.A., Heeger, A.J., and Plaxco, K.W. (2005). *Angew. Chem. Int. Ed.* 44: 5456–5459.

72 Baker, B.R., Lai, R.Y., Wood, M.S. et al. (2006). *J. Am. Chem. Soc.* 128: 3138–3139.
73 Vallée-Bélisle, A., Ricci, F., Uzawa, T. et al. (2012). *J. Am. Chem. Soc.* 134: 15197–15200.
74 Mahshid, S.S., Camiré, S., Ricci, F., and Vallée-Bélisle, A. (2015). *J. Am. Chem. Soc.* 137: 15596–15599.
75 Kang, D., White, R.J., Xia, F. et al. (2012). *NPG Asia Mater.* 4: e1.
76 Katz, E. and Willner, I. (2003). *Electroanalysis* 15: 913–947.
77 Bardea, A., Patolsky, F., Dagan, A., and Willner, I. (1999). *Chem. Commun.*: 21–22.
78 Fan, D., Fan, Y., Wang, E., and Dong, S. (2018). *Chem. Sci.* 9: 6981–6987.
79 Li, W., Nie, Z., Xu, X. et al. (2009). *Talanta* 78: 954–958.
80 Zayats, M., Huang, Y., Gill, R. et al. (2006). *J. Am. Chem. Soc.* 128: 13666–13667.
81 Gao, W., Zhang, L., Zhang, Y.-M. et al. (2014). *J. Phys. Chem. C* 118: 14410–14417.
82 Freeman, R., Liu, X., and Willner, I. (2011). *J. Am. Chem. Soc.* 133: 11597–11604.
83 Kim, N.H., Lee, S.J., and Moskovits, M. (2010). *Nano Lett.* 10: 4181–4185.
84 Simon, A.J., Vallée-Bélisle, A., Ricci, F. et al. (2014). *Angew. Chem. Int. Ed.* 53: 9471–9475.
85 Porchetta, A., Vallée-Bélisle, A., Plaxco, K.W., and Ricci, F. (2012). *J. Am. Chem. Soc.* 134: 20601–20604.
86 Porchetta, A., Vallée-Bélisle, A., Plaxco, K.W., and Ricci, F. (2013). *J. Am. Chem. Soc.* 135: 13238–13241.
87 Buchler, N.E. and Cross, F.R. (2009). *Mol. Syst. Biol.* 5: 272.
88 Buchler, N.E. and Louis, M. (2008). *J. Mol. Biol.* 384: 1106–1119.
89 Ricci, F., Vallée-Bélisle, A., and Plaxco, K.W. (2011). *PLoS Comput. Biol.* 7: e1002171.
90 Fadel, T.R., Farrell, D.F., Friedersdorf, L.E. et al. (2016). *ACS Sens.* 1: 207–216.
91 Gupta, S., Hirota, M., Waugh, S.M. et al. (2014). *J. Biol. Chem.* 289: 8706–8719.
92 Drolet, D.W., Green, L.S., Gold, L., and Janjic, N. (2016). *Nucleic Acid Ther.* 26: 127–146.
93 Bamrungsap, S., Zhao, Z., Chen, T. et al. (2012). *Nanomedicine* 7: 1253–1271.
94 Tørring, T. and Gothelf, K.V. (2013). *F1000Prime Rep.* 5: 14.